

ANTISYMMETRIC AND SYMMETRIC FUNCTIONALLY GRADED PLATE-TYPE STRUCTURES IMPACTED BY BLAST LOADING

Terry Hause, Ph.D.

Research Mechanical Engineer
U.S. Army RDECOM-TARDEC
Warren, MI 48397

Sudhakar, Arepally

Deputy Associate Director
U.S. Army RDECOM-TARDEC
Warren, MI 48397

ABSTRACT

The foundation of the theory of functionally graded plates with simply supported edges, under a Friedlander explosive air-blast, are developed within the classical plate theory (CPT). Within the development of the theory, the two constituent phases, ceramic and metal, vary across the wall thickness according to a prescribed power law. The theory includes the geometrical nonlinearities, the dynamic effects, compressive tensile edge loadings, and the damping effects. Also presented are the analytical expressions for the stresses, in which the results of which are not presented here. The static and dynamic solutions are developed leveraging the use of a stress potential with the Extended-Galerkin method and the Runge-Kutta method. The analysis focuses on how to alleviate the effects of large deformations through proper material selection and the proper gradation of the constituent phases or materials.

1. INTRODUCTION

During combat situations, the structure of army military vehicles may have to structurally endure the effects of blast loading. Advances in functionally graded materials (FGM's) which combine the properties of two dissimilar materials has been a motivating factor in viewing these types of materials as a viable alternative to the current isotropic metallic structures being utilized in the hull and armor plating. FGM's are microscopically inhomogeneous with thermo-mechanical properties which vary smoothly and continuously from one surface to another. These graded structures allow the integration of dissimilar materials like ceramic and metals that combine different or even incompatible properties such as hardness and toughness.

In this paper, the foundation of the nonlinear theory of functionally graded plate-type structures under an explosive air-blast is developed. An approximate solution methodology for the intricate nonlinear boundary value problem is devised, and results that are likely to contribute to a better understanding of the structural behavior, under an explosive blast with beneficial implications towards their improved design and exploitation are presented. It is the author's intent, within

this paper, to fill in some major gaps currently existing within the specialized literature.

2. BASIC ASSUMPTIONS AND PRELIMINARIES

The plate mid surface is referred to a cartesian orthogonal system of coordinates (x,y,z), while z is the thickness coordinate measured positive in the upwards direction from the mid-surface of the plate with h being the uniform plate thickness and y is directed perpendicular to the x-axis in the plane of the plate. See figure 1 below.

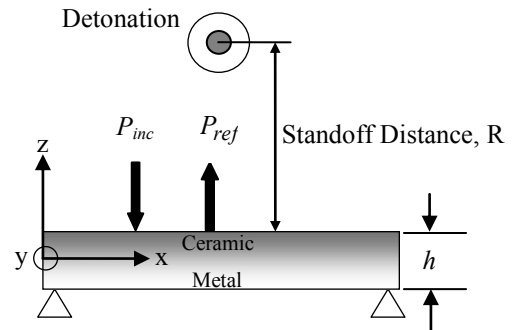


Figure 1: A simply supported functionally graded plate Shown in 2-D, under an explosive blast.

Report Documentation Page			Form Approved OMB No. 0704-0188		
Public reporting burden for the collection of information is estimated to average 1 hour per response, including the time for reviewing instructions, searching existing data sources, gathering and maintaining the data needed, and completing and reviewing the collection of information. Send comments regarding this burden estimate or any other aspect of this collection of information, including suggestions for reducing this burden, to Washington Headquarters Services, Directorate for Information Operations and Reports, 1215 Jefferson Davis Highway, Suite 1204, Arlington VA 22202-4302. Respondents should be aware that notwithstanding any other provision of law, no person shall be subject to a penalty for failing to comply with a collection of information if it does not display a currently valid OMB control number.					
1. REPORT DATE 13 SEP 2010	2. REPORT TYPE N/A	3. DATES COVERED -			
4. TITLE AND SUBTITLE Antisymmetric and Symmetric Functionally Graded Plate-Type Structures Impacted by Blast Loading		5a. CONTRACT NUMBER			
		5b. GRANT NUMBER			
		5c. PROGRAM ELEMENT NUMBER			
6. AUTHOR(S) Terry Hause, Ph.D.; Sudhakar, Arepally		5d. PROJECT NUMBER			
		5e. TASK NUMBER			
		5f. WORK UNIT NUMBER			
7. PERFORMING ORGANIZATION NAME(S) AND ADDRESS(ES) US Army RDECOM-TARDEC 6501 E 11 Mile Rd Warren, MI 48397-5000, USA		8. PERFORMING ORGANIZATION REPORT NUMBER 21171			
9. SPONSORING/MONITORING AGENCY NAME(S) AND ADDRESS(ES)		10. SPONSOR/MONITOR'S ACRONYM(S) TACOM/TARDEC			
		11. SPONSOR/MONITOR'S REPORT NUMBER(S) 21171			
12. DISTRIBUTION/AVAILABILITY STATEMENT Approved for public release, distribution unlimited					
13. SUPPLEMENTARY NOTES Presented at the 27th Army Science conference (ASC), 29 November 2 December 2010 Orlando, Florida, USA					
14. ABSTRACT The foundation of the theory of functionally graded plates with simply supported edges, under a Friedlander explosive air-blast, are developed within the classical plate theory (CPT). Within the development of the theory, the two constituent phases, ceramic and metal, vary across the wall thickness according to a prescribed power law. The theory includes the geometrical nonlinearities, the dynamic effects, compressive tensile edge loadings, and the damping effects. Also presented are the analytical expressions for the stresses, in which the results of which are not presented here. The static and dynamic solutions are developed leveraging the use of a stress potential with the Extended-Galerkin method and the Runge-Kutta method. The analysis focuses on how to alleviate the effects of large deformations through proper material selection and the proper gradation of the constituent phases or materials.					
15. SUBJECT TERMS					
16. SECURITY CLASSIFICATION OF:			17. LIMITATION OF ABSTRACT SAR	18. NUMBER OF PAGES 8	19a. NAME OF RESPONSIBLE PERSON
a. REPORT unclassified	b. ABSTRACT unclassified	c. THIS PAGE unclassified			

The nonlinear elastic theory of Functionally Graded (FG) Plates is developed using the classical plate deformation Theory [6]. It is also assumed that the FG plate is made-up of ceramic and metal phases whose material properties vary smoothly and continuously across the wall thickness. By applying the rule of mixtures, the material properties such as Young's Modulus, Density, and Poisson's Ratio are assumed to vary across the wall thickness as

$$P(z) = P_c V_c(z) + P_m V_m(z), \quad (1)$$

In which P_c and P_m denote the material properties of the ceramic and metallic phases, of the plate, respectively.

$V_c(z)$ and $V_m(z)$ are correspondingly, the volume fractions of the ceramic and metal respectively, fulfilling the relation

$$V_c(z) + V_m(z) = 1. \quad (2)$$

By virtue of (2), Eq. (1a) can be expressed as

$$P(z) = (P_c - P_m)V_c(z) + P_m. \quad (3)$$

Two Scenarios of the grading of the two basic component phases, ceramic and metal, through the wall thickness are considered.

Case (1): The phases vary symmetrically through the wall thickness, in the sense of having full ceramic at the outer surfaces of the plate and tending toward full metal at the mid-surface. For this case,

$$V_c(z) = \left(\frac{z}{h/2}\right)^N \left(\frac{1 + \text{sgn}(z)}{2}\right) + \left(\frac{-z}{h/2}\right)^N \left(\frac{1 - \text{sgn}(z)}{2}\right) \quad (4)$$

Where the signum function, $\text{sgn}(z)=1$, $z>0$, 0 , $z=0$, and -1 , $z<0$.

N is termed the volume fraction index which provides the material variation profile through the plate wall thickness, ($0 \leq N \leq \infty$).

Case (2): The phases vary non-symmetrically through the wall thickness, and in this case there is full ceramic at the outer surface of the plate wall and full metal at its inner surface. For this case, $V_c(z)$ can be expressed as

$$V_c(z) = \left(\frac{h + 2z}{2h}\right)^N \quad (5)$$

It should be noted that in contrast to case (2), where there exists coupling between stretching and bending, such coupling is not present for the symmetric case (1).

Also, for the purposes of simplicity the Poisson's ratio will be assumed to be constant throughout the plate structure.

3. KINEMATIC EQUATIONS

3.1 The 3-D Displacement Field

Consistent with the classical plate theory [6], the distribution of the 3-D

$$\begin{aligned} u(x, y, z, t) &= u_0(x, y, t) - z \frac{\partial w_0(x, y, t)}{\partial x}, \\ v(x, y, z, t) &= v_0(x, y, t) - z \frac{\partial w_0(x, y, t)}{\partial y}, \\ w(x, y, z, t) &= w_0(x, y, t) \end{aligned} \quad (6a-c)$$

Within these equations, (u, v, w) are the 3-D displacement quantities along the (x, y, z) directions, respectively. While, u_0, v_0 , and w_0 are the 2-D displacement quantities of the points on the mid-surface.

3.2 NonLinear Strain Displacement Relationships

The nonlinear strain displacement relationships across the plate thickness at a distance from the mid-surface take the form

$$\begin{Bmatrix} \varepsilon_{xx} \\ \varepsilon_{yy} \\ \gamma_{xy} \end{Bmatrix} = \begin{Bmatrix} \varepsilon_{xx}^{(0)} \\ \varepsilon_{yy}^{(0)} \\ \gamma_{xy}^{(0)} \end{Bmatrix} + z \begin{Bmatrix} \varepsilon_{xx}^{(1)} \\ \varepsilon_{yy}^{(1)} \\ \gamma_{xy}^{(1)} \end{Bmatrix} \quad (7)$$

Where,

$$\{\varepsilon^{(0)}\} = \begin{Bmatrix} \varepsilon_{xx}^{(0)} \\ \varepsilon_{yy}^{(0)} \\ \gamma_{xy}^{(0)} \end{Bmatrix} = \begin{Bmatrix} \frac{\partial u_0}{\partial x} + \frac{1}{2} \left(\frac{\partial w_0}{\partial x} \right)^2 \\ \frac{\partial v_0}{\partial x} + \frac{1}{2} \left(\frac{\partial w_0}{\partial y} \right)^2 \\ \frac{\partial u_0}{\partial y} + \frac{\partial v_0}{\partial x} + \frac{\partial w_0}{\partial x} \frac{\partial w_0}{\partial y} \end{Bmatrix},$$

$$\{\varepsilon^{(1)}\} = \begin{Bmatrix} \varepsilon_{xx}^{(1)} \\ \varepsilon_{yy}^{(1)} \\ \gamma_{xy}^{(1)} \end{Bmatrix} = \begin{Bmatrix} -\frac{\partial^2 w_0}{\partial x^2} \\ -\frac{\partial^2 w_0}{\partial y^2} \\ -2 \frac{\partial^2 w_0}{\partial x \partial y} \end{Bmatrix}$$

In the above expressions, $(\varepsilon_{xx}^0, \varepsilon_{yy}^0, \gamma_{xy}^0)$, are referred to as the membrane strains and $(\varepsilon_{xx}^1, \varepsilon_{yy}^1, \gamma_{xy}^1)$ are referred to as the flexural bending strains which are also known as the curvatures.

4. CONSTITUTIVE EQUATIONS

The stress-strain relationships for a state of plane stress is expressed as [10]

$$\begin{Bmatrix} \sigma_{xx} \\ \sigma_{yy} \\ \sigma_{xy} \end{Bmatrix} = \begin{bmatrix} Q_{11} & Q_{12} & 0 \\ Q_{12} & Q_{22} & 0 \\ 0 & 0 & Q_{66} \end{bmatrix} \begin{Bmatrix} \varepsilon_{xx} \\ \varepsilon_{yy} \\ \gamma_{xy} \end{Bmatrix}$$

$$\sigma_{xz} = \sigma_{yz} = \sigma_{zz} = 0 \quad (8)$$

The material stiffnesses, $Q_{ij}(z)$, ($i = 1, 2, 6$) are given by [9, 10]

$$Q_{11} = Q_{22} = \frac{E(z)}{1 - \nu^2}, \quad Q_{12} = \frac{\nu E(z)}{1 - \nu^2},$$

$$Q_{66}(z) = \frac{E(z)}{2(1 + \nu)}, \quad (Q_{16}, Q_{26}) = 0 \quad (9)$$

The standard force and moment resultants of a plate are defined as

$$(N_{ij}, M_{ij}) = \int_{-h/2}^{h/2} \sigma_{ij}(1, z) dz, \quad (i, j = x, y, xy) \quad (10)$$

With the use of Equations (7)–(10), the stress resultants and stress couples are related to the strains by [3]

$$\begin{Bmatrix} N \\ M \end{Bmatrix} = \begin{bmatrix} [A] & [B] \\ [B] & [D] \end{bmatrix} \begin{Bmatrix} \varepsilon^{(0)} \\ \varepsilon^{(1)} \end{Bmatrix}, \quad (11)$$

In which $[A]$, $[B]$, and $[D]$ are the respective in-surface, bending-stretching coupling, and bending stiffnesses. For the case of symmetric FG Plates, $[B] = 0$, since there is no bending-stretching coupling. The global stiffness quantities, A_{ij} , B_{ij} , and D_{ij} , ($i, j = 1, 2, 6$) are defined as

$$(A_{ij}, B_{ij}, D_{ij}) = \int_{-h/2}^{h/2} Q_{ij}(1, z, z^2) dz, \quad (i, j = 1, 2, 6) \quad (12)$$

In view of Equations (3), (4), (5), (9), and (12), the global stiffness quantities are determined as

$$[(A_{11}, A_{22}), (B_{11}, B_{22}), (D_{11}, D_{22})] = \frac{1}{1 - \nu^2} (E_1, E_2, E_3),$$

$$(A_{12}, B_{12}, D_{12}) = \frac{\nu}{1 - \nu^2} (E_1, E_2, E_3),$$

$$(A_{66}, B_{66}, D_{66}) = \frac{1}{2(1 + \nu)} (E_1, E_2, E_3) \quad (13a-c)$$

where for the asymmetric case,

$$E_1 = \frac{E_{cm} h}{N + 1} + E_{cm} h, \quad E_2 = \frac{E_{cm} h^2}{N + 2} - \frac{E_{cm} h^2}{2N + 2},$$

$$E_3 = E_{cm} h^3 \left(\frac{1}{N + 3} - \frac{1}{N + 2} + \frac{1}{4N + 4} \right) + \frac{E_m h^3}{12} \quad (14)$$

And for the symmetric case,

$$E_1 = \frac{E_{cm} h}{N + 1} + E_{cm} h, \quad E_2 = 0, \quad E_3 = \frac{E_{cm} h^3}{4(N + 3)} + \frac{E_m h^3}{12} \quad (15)$$

5. GOVERNING EQUATIONS

Hamilton's principle is used to derive the equations of motion and the boundary conditions. It is formulated as

$$\delta J = \delta \int_{t_0}^{t_1} (U + V - K) dt = 0, \quad (16)$$

Where t_0 and t_1 are two arbitrary instants of time. U denotes the strain energy, V denotes the work done by surface tractions, edge loads, and body forces, and K denotes the kinetic energy of the 3-D body of the structure, while δ is the variational operator. In Equation (16), the strain energy is given by

$$\delta U = \int_{\Omega_0} \left[\int_{-\frac{h}{2}}^{\frac{h}{2}} (\sigma_{xx} \delta \varepsilon_{xx} + \sigma_{yy} \delta \varepsilon_{yy} + \sigma_{xy} \delta \gamma_{xy}) dz \right] d\Omega_0 \quad (17)$$

where Ω_0 denotes the mid-surface area of the panel. The work done by external loads is expressed as

$$\delta V = - \int_{\Omega_0} \left[P_t(x, y) \delta w \left(x, y, \frac{h}{2} \right) - P_b(x, y) \delta w \left(x, y, -\frac{h}{2} \right) \right] d\Omega_0$$

$$- \int_x \int_{-\frac{h}{2}}^{\frac{h}{2}} (\sigma_{yy}^* \delta v + \sigma_{yx}^* \delta u) dz dx - \int_y \int_{-\frac{h}{2}}^{\frac{h}{2}} (\sigma_{xx}^* \delta u + \sigma_{xy}^* \delta v) dz dy \quad (18)$$

In the above expression, $P_t(x, y)$ is the distributed force at the top surface ($z = h/2$), $P_b(x, y)$ is the distributed

force at the bottom surface ($z = -h/2$), $(\sigma_{xx}^*, \sigma_{yy}^*, \sigma_{xy}^*, \sigma_{yx}^*)$ are the specified stress components along the plate edges, and $(\delta u, \delta v)$ are the virtual displacements along the normal and tangential directions, respectively, along the plate edges. Considering only the transversal inertia of the structure, the kinetic energy is given by

$$K = \frac{1}{2} \int_V \rho_0(z) \dot{W}^2 dV, \quad (19)$$

Which implies that the variation in kinetic energy is expressed as

$$\delta K = \int_{\Omega_0} \int_{-\frac{h}{2}}^{\frac{h}{2}} \rho(z) \dot{W} \delta \dot{W} dz d\Omega_0 \quad (20)$$

where $\rho(z)$ is the mass per unit volume.

Considering Equation (16) in conjunction with Equations (17)-(20), along with the constitutive equations (8), the strain-displacement relationships, equations (7), and carrying out the integration through the thickness, integrating by parts whenever feasible, using the expression of global stress resultants and stress couples, while retaining only the transversal load, transverse inertia, and transverse damping, invoking the arbitrary and independent character of variations

$\delta u_0, \delta v_0, \delta w_0, \delta(\partial w_0/\partial x)$, and $\delta(\partial w_0/\partial y)$ one obtains the equations of motion and as a by-product the boundary terms or conditions. This results in three equations of motion in terms of the global stress resultants and stress couples and the four boundary conditions along the plate edges. These equations of motion and boundary conditions can be respectively expressed as

$$\delta u_0 : \quad \frac{\partial N_{xx}}{\partial x} + \frac{\partial N_{xy}}{\partial y} = 0 \quad (21a)$$

$$\delta v_0 : \quad \frac{\partial N_{yy}}{\partial y} + \frac{\partial N_{xy}}{\partial x} = 0 \quad (21b)$$

$$\begin{aligned} & \frac{\partial^2 M_{xx}}{\partial x^2} + 2 \frac{\partial^2 M_{xy}}{\partial x \partial y} + \frac{\partial^2 M_{yy}}{\partial y^2} + \frac{\partial}{\partial x} \left(N_{xx} \frac{\partial w_0}{\partial x} \right. \\ & \left. + N_{xy} \frac{\partial w_0}{\partial y} \right) + \frac{\partial}{\partial y} \left(N_{xy} \frac{\partial w_0}{\partial y} + N_{yy} \frac{\partial w_0}{\partial x} \right) + P_t \\ & - C \dot{w}_0 = I_0 \ddot{w}_0 \end{aligned} \quad (21c)$$

For the case of all edges simply supported and freely movable the boundary conditions are as follows:

$$\begin{aligned} w_0 = M_{xx} = N_{xy} = 0, N_{xx} = N_{xx}^* \text{ on } x = 0, L_1 \\ w_0 = M_{yy} = N_{yx} = 0, N_{yy} = N_{yy}^* \text{ on } y = 0, L_2 \end{aligned} \quad (22)$$

It should be mentioned for clarification sake that for compressive edge loading $N_{xx}^* = -N_{xx}^0$, and $N_{yy}^* = -N_{yy}^0$.

6. AIR-BLAST LOADING

With the ever increasing demands for increased safety for the soldiers in the field to operate structurally sound vehicles in the event of an improvised explosive device (IED) or some other type of explosive, it is imperative that an understanding of the structural response of various components within military combat vehicles under an explosive blast be understood so that measures can be taken from a design standpoint to ensure the durability and survivability of these components. To begin to achieve this understanding, the type of explosive loading considered here is a free in-air spherical air burst. Such an explosion creates a spherical shock wave which travels radially outward in all directions with diminishing velocity. The mathematical expression representing the incident blast wave from a spherical charge is given by

$$P_t(t) = (P_{S0} - P_0) \left(1 - \frac{t - t_a}{t_p} \right) e^{-\alpha \left(\frac{t - t_a}{t_p} \right)} \quad (23)$$

Where

$$P_{S0} = \frac{1772}{Z^3} - \frac{114}{Z^2} + \frac{108}{Z} \quad (24)$$

P_{S0} is the peak overpressure above ambient pressure, P_0 is the ambient pressure, t_a is the time of arrival, t_p is the positive phase duration of the blast wave, and t is the time. The waveform shown in figure 4 is

In equations (23) and (24) Z is known as the scaled distance given by $Z = R/W^{1/3}$ with R being the standoff distance in meters and W being the equivalent charge weight of TNT in terms of kilograms. Also, α is known as the decay parameter which is determined by adjustment to a pressure curve from a blast test.

For the conditions of standard temperature and pressure (STP) at sea level, the time of arrival t_a , and the positive phase duration t_p , can be determined from [4]

$$\frac{t}{t_1} = \frac{R}{R_1} = \left(\frac{W}{W_1} \right)^{\frac{1}{3}} \quad (25)$$

Where t_1 represents either the arrival time or positive phase duration for a reference explosion of charge weight W_1 , and t represents either the arrival time or positive phase duration for any explosion of charge weight W . The determination of the standoff distance for any charge weight W follows a similar reasoning. The application of these relationships is known as cube root scaling. It should be understood that in applying these relationships that the standoff distances are themselves scaled according to the cube root law.

7. SOLUTION METHODOLOGY

To satisfy the first two equations of motion, equations (31a,b), a stress potential will be utilized which allows the in-plane stress resultants to be expressed by letting

$$N_{xx} = \frac{\partial^2 \phi}{\partial y^2}, N_{yy} = \frac{\partial^2 \phi}{\partial x^2}, N_{xy} = -\frac{\partial^2 \phi}{\partial x \partial y}. \quad (26)$$

The third equation of motion, equation (21c), can be expressed in terms of two unknown variables, the stress potential ϕ and the transverse displacement w_0 which results in

$$D \nabla^4 w_0 - \left(\frac{\partial^2 \phi}{\partial x^2} \frac{\partial^2 w_0}{\partial y^2} - 2 \frac{\partial^2 \phi}{\partial x \partial y} \frac{\partial^2 w_0}{\partial x \partial y} + \frac{\partial^2 \phi}{\partial y^2} \frac{\partial^2 w_0}{\partial x^2} \right) + \quad (27a)$$

$$I_0 \ddot{w}_0 + C \dot{w}_0 = P_t + \theta \nabla^2 N^T + \nabla^2 M^T$$

Where,

$$D = \frac{E_1 E_3 - E_2^2}{E_1 (1 - \nu^2)}, \quad \theta = -\frac{E_2}{E_1} \quad (27b,c)$$

This gives one governing equation with two unknowns, w_0 and ϕ . One more equation is needed in terms of the same unknowns which will give two equations in terms of two unknowns which can then be solved. This will come from the compatibility equation. By eliminating the in-plane displacements from the strain-displacement relationships, equations (7) the relationship between the in-plane strains and the transversal deflection known as the compatibility equation can be shown to be given by

$$\frac{\partial^2 \epsilon_{xx}^0}{\partial y^2} + \frac{\partial^2 \epsilon_{yy}^0}{\partial x^2} - \frac{\partial^2 \gamma_{xy}^0}{\partial x \partial y} = \left(\frac{\partial^2 w_0}{\partial x \partial y} \right)^2 - \frac{\partial^2 w_0}{\partial x^2} \frac{\partial^2 w_0}{\partial y^2} \quad (28)$$

Which, in terms of ϕ and w_0 , becomes

$$\nabla^4 \phi = E_1 \left[\left(\frac{\partial^2 w_0}{\partial x \partial y} \right)^2 - \frac{\partial^2 w_0}{\partial x^2} \frac{\partial^2 w_0}{\partial y^2} \right] - (1 - \nu) \nabla^2 N^T \quad (29)$$

In equations (27) and (29), $\nabla^2 = \partial^2 / \partial x^2 + \partial^2 / \partial y^2$ where ∇ is referred to as the Laplacian operator.

Equations (27a) and (29) are the basic governing equations used to investigate the structural response of FG plates under external excitation loading. For the purposes of this paper, from this point forward, the thermal terms will be discarded. To this end, to solve equations (27a) and (29), the approach adopted from [2] will be utilized. In this respect, the following functional forms are assumed for w_0 and ϕ [2].

$$w_0(x, y, t) = w_{mn}(t) \sin \lambda_m x \sin \mu_n y \quad (30a,b)$$

$$\begin{aligned} \phi = & A_{mn}(t) \cos 2\lambda_m x + B_{mn}(t) \cos 2\mu_n y + \\ & C_{mn}(t) \cos 2\lambda_m x \cos 2\mu_n y + D_{mn}(t) \sin 2\lambda_m x \sin 2\mu_n y + \\ & \frac{1}{2} N_{xx}^* y^2 + \frac{1}{2} N_{yy}^* x^2 \end{aligned}$$

Where $\lambda_m = m\pi/L_1$, $\mu_n = n\pi/L_2$, $m, n = 1, 2, \dots$ are the number of half waves in the x and y directions, respectively, and $w_{mn}(t)$ is the amplitude of deflection. Also, $A_{mn}(t)$, $B_{mn}(t)$, $C_{mn}(t)$, and $D_{mn}(t)$ are coefficients to be determined. By substituting equations (50a,b) into equation (49), the coefficients $A_{mn}(t)$, $B_{mn}(t)$, $C_{mn}(t)$, and $D_{mn}(t)$ are determined as

$$\begin{aligned} A_{mn}(t) &= \frac{E_1 w_{mn}^2(t) \mu_n^2}{32 \lambda_m^2}, B_{mn}(t) = \frac{E_1 w_{mn}^2(t) \lambda_n^2}{32 \mu_m^2}, \\ C_{mn}(t) &= D_{mn}(t) = 0 \end{aligned} \quad (31)$$

By letting,

$$P_t(t) = P_{mn}(t) \sin \lambda_m x \sin \mu_n y \quad (32)$$

And integrating both sides over the plate area gives

$$P_{mn}(t) = \frac{16 P_t(t)}{\pi^2}, \quad (m, n) = (1, 1) \quad (33)$$

and introduction of equations (30a,b) and (31) into equation (27a) and retaining the resulting equation along with the unsatisfied boundary conditions in the energy functional and applying the Extended Galerkin technique results in the following nonlinear differential equation

governing the structural response of FG plates, under external excitation.

$$\ddot{w}_{mn}(t) + 2\Delta_{mn}\omega_{mn}\dot{w}_{mn}(t) + \omega_{mn}^2 w_{mn}(t) + \Omega_{mn}(t)w_{mn}^3(t) = \tilde{P}_{mn}(t) \quad (34)$$

Where, $w_{mn}(t)$ represents the amplitude of deflection of the plate as a function of time. The expressions for ω_{mn} , Δ_{mn} , Ω_{mn} , and \tilde{P}_{mn} are not provided here.

Equation (34) is a nonlinear equation in terms of the plate deflections as a function of time. To obtain the plate deflections as a function of time, equation (34) is solved using the Fourth-Order Runge-Kutta Method.

8. MECHANICAL STRESS ANALYSIS

With the transversal deflections in hand, as a function of time, the plane stresses can be determined from the constitutive equations (8) with the use of the strain-displacement relationships, equations (7) and the stiffness equations, equation (9) results in,

$$\sigma_{xx} = \frac{E(z)}{1-\nu^2} \left[\frac{\partial u_0}{\partial x} + \nu \frac{\partial v_0}{\partial y} + \frac{1}{2} \left(\frac{\partial w_0}{\partial x} \right)^2 + \frac{\nu}{2} \left(\frac{\partial w_0}{\partial y} \right)^2 - z \left(\frac{\partial^2 w_0}{\partial x^2} + \nu \frac{\partial^2 w_0}{\partial y^2} \right) \right] \quad (35a)$$

$$\sigma_{yy} = \frac{E(z)}{1-\nu^2} \left[\frac{\partial v_0}{\partial y} + \nu \frac{\partial u_0}{\partial x} + \frac{1}{2} \left(\frac{\partial w_0}{\partial y} \right)^2 + \frac{\nu}{2} \left(\frac{\partial w_0}{\partial x} \right)^2 - z \left(\frac{\partial^2 w_0}{\partial y^2} + \nu \frac{\partial^2 w_0}{\partial x^2} \right) \right] \quad (35b)$$

$$\sigma_{xy} = \frac{E(z)}{2(1+\nu)} \left[\frac{\partial u_0}{\partial y} + \frac{\partial v_0}{\partial x} + \frac{\partial w_0}{\partial x} \frac{\partial w_0}{\partial y} - 2z \frac{\partial^2 w_0}{\partial x \partial y} \right] \quad (35c)$$

In order to determine the stresses, the expressions for u_0 and v_0 in terms of the transversal amplitude of deflection, $w_{mn}(t)$ needs to be determined. These relationships can be determined from the global constitutive equations (11). Expanding equation (11) gives,

$$\begin{aligned} N_{xx} &= A_{11}\varepsilon_{xx}^{(0)} + A_{12}\varepsilon_{yy}^{(0)} + B_{11}\varepsilon_{xx}^{(1)} + B_{12}\varepsilon_{yy}^{(1)} \\ N_{yy} &= A_{12}\varepsilon_{xx}^{(0)} + A_{22}\varepsilon_{yy}^{(0)} + B_{12}\varepsilon_{xx}^{(1)} + B_{22}\varepsilon_{yy}^{(1)} \end{aligned} \quad (36a,b)$$

Solving Equations (36a,b) simultaneously for $\varepsilon_{xx}^{(0)}$, and $\varepsilon_{yy}^{(0)}$ in terms of N_{xx} , N_{yy} , $\varepsilon_{xx}^{(1)}$, and $\varepsilon_{yy}^{(1)}$ and utilizing equations (7) and (26) gives,

$$\begin{aligned} \frac{\partial v_0}{\partial y} &= \left(\frac{A_{11}}{A_{12}^2 - A_{11}A_{22}} \right) \frac{\partial^2 \varphi}{\partial x^2} + \left(\frac{-A_{12}}{A_{12}^2 - A_{11}A_{22}} \right) \frac{\partial^2 \varphi}{\partial y^2} - \\ &\left(\frac{A_{12}B_{11} - A_{11}B_{12}}{A_{12}^2 - A_{11}A_{22}} \right) \frac{\partial^2 w_0}{\partial x^2} - \left(\frac{A_{12}B_{12} - A_{11}B_{22}}{A_{12}^2 - A_{11}A_{22}} \right) \frac{\partial^2 w_0}{\partial y^2} \\ &- \frac{1}{2} \left(\frac{\partial w_0}{\partial y} \right)^2 \\ \frac{\partial u_0}{\partial x} &= \left(\frac{-A_{12}}{A_{12}^2 - A_{11}A_{22}} \right) \frac{\partial^2 \varphi}{\partial x^2} + \left(\frac{A_{22}}{A_{12}^2 - A_{11}A_{22}} \right) \frac{\partial^2 \varphi}{\partial y^2} - \\ &\left(\frac{A_{12}B_{12} - A_{22}B_{11}}{A_{12}^2 - A_{11}A_{22}} \right) \frac{\partial^2 w_0}{\partial x^2} - \left(\frac{A_{12}B_{22} - A_{22}B_{12}}{A_{12}^2 - A_{11}A_{22}} \right) \frac{\partial^2 w_0}{\partial y^2} \\ &- \frac{1}{2} \left(\frac{\partial w_0}{\partial x} \right)^2 \end{aligned} \quad (37a,b)$$

With the use of equations (13a-c), (30a,b), and (31) and integrating equations (37a,b), u_0 and v_0 can be determined. Having in hand, the expressions for u_0 , v_0 , and w_0 , the expressions for the stress distribution can be determined from equations (35a-c).

9. RESULTS AND DISCUSSION

To illustrate the present approach, a ceramic-metal functionally graded plate consisting of Ti-6Al-4V and Aluminum Oxide with the following material properties, which were adopted from [9], were considered for the numerical results presented.

$$\begin{aligned} E_c &= 320.24 \text{ GPa}, & \rho_c &= 3750 \text{ kg/m}^3, & \nu_c &= 0.26 \\ E_m &= 105.7 \text{ GPa}, & \rho_m &= 4429 \text{ kg/m}^3, & \nu_m &= 0.2981 \\ & & \nu_{ave} &= 0.2791 \end{aligned}$$

The geometrical properties used for the FG Plate are $L_1 = 1 \text{ m}$, $\psi = L_1/L_2 = 1.25$, and unless otherwise stated $h = 0.0254 \text{ m}$ and the halfwaves, $(m,n) = (1,1)$. In

addition, the following reference values, in Table 1. were utilized to determine the time of arrival and positive phase duration [5].

Table 1. Airblast Parameters Versus Distance for a One Kilogram (W_1) TNT Spherical Air Burst [5].

Standoff Distance, R_1 (m)	Arrival Time, t_{a1} (msec)	Positive Phase Duration, t_{p1} (msec)
1.0	0.532	1.79

In Fig. 2 below, comparisons are made between the deflections of an asymmetric and symmetric plate. It can be seen that the deflections are a little out of phase with each other. Also, the symmetric FG plate has slightly lower deflections for a volume fraction index of 0.1. As can also be seen, that for a fixed amount of damping, the deflections are attenuated rather quickly.

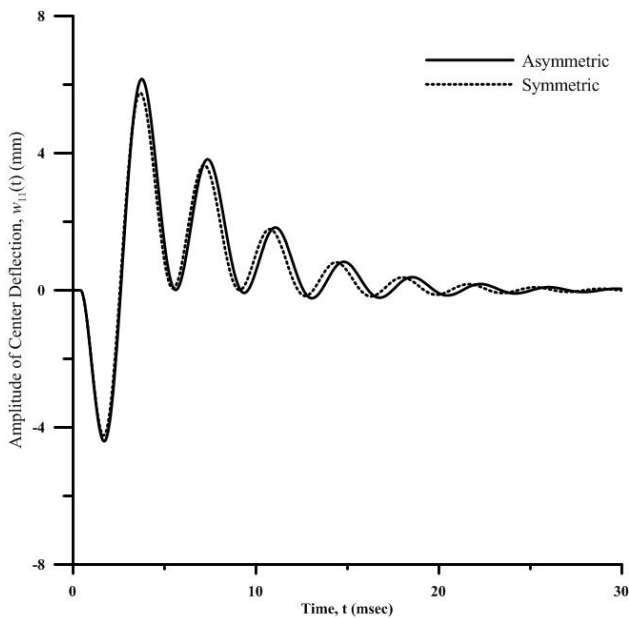


Fig. 2 . Implications of the symmetry on the central deflection as function of time. ($N=0.1$, $\Delta_1=0.1$)

In Fig. 3, It is shown for an asymmetric FG plate, that as the volume fraction index increases from a value of zero (fully ceramic) to a value of 10 (essentially fully metal) that the deflections increase then taper off as phases of the constituent materials approach fully metal. This shows that metal have higher deflections than the ceramic implying that the grading of the FG plate plays an important role.

In Fig. 4, which is the counterpart of Fig. 3 for a symmetric FG plate, reveals similar behavior. As mentioned earlier symmetric FG plates have lower

deflections than asymmetric FG plates. Also, it can be seen that damping attenuates the deflections very rapidly.

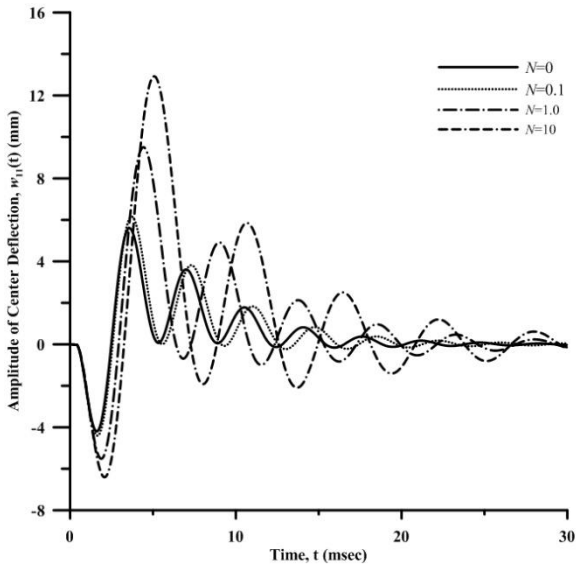


Fig. 3 . Implications of the volume fraction index on the central deflection as a function of time on an asymmetric functionally graded plate. ($\Delta_1=0.1$)

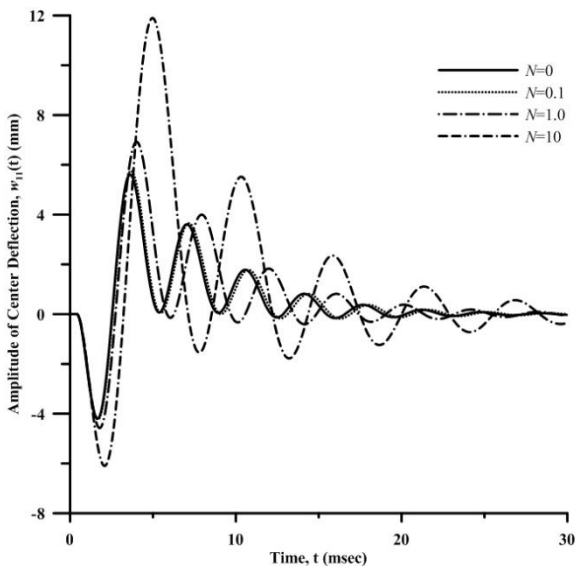


Fig. 4. Implications of the volume fraction index on the central deflection as a function of time on an symmetric functionally graded plate. ($\Delta_1=0.1$)

10. CONCLUDING REMARKS

A rigorous treatment of functionally graded plates with grading in the transverse direction has been studied. It has been shown that damping has an important effect when it comes to the attenuation of the deflections. It has also been shown that the symmetry of the transverse grading throughout the structure plays an important role in the deflection-time history of the structure.

From a design standpoint, it would be appropriate at this point to state that integration of functionally graded materials within plate-type structures would benefit the structural response of the structure. Also, it should be mentioned, although not shown here, that the choice of the ceramic and metal constituent materials chosen would also have a great impact on the response of the structure.

The idea is to reduce the stresses within the structure concerned here. By reducing the magnitude of the deflections, the stresses are reduced. It is hoped and realized that this present study presented here will give insight into some of the factors that can play an important role in the structural response of functionally graded plates and fill in some of the fundamental missing gaps within this subject area.

FUTURE WORK

It should be noted that further work should and needs to be explored which would address comparing finite element blast modeling and simulation results with the current analytical results based on the theory of elasticity. This can be accomplished, by exploring the implementation of these analytical equations, as a user subroutine, in one of the applicable software tools.

ACKNOWLEDGEMENTS

The author would like to express thanks to the U.S. Army-RDECOM-TARDEC for their support and funding under the Independent Laboratory In-house Research program (IL

REFERENCES

- [1] Akay, H.U., "Dynamic Large Deflection Analysis of Plates Using Mixed Finite Elements", *Computers and Structures*, Vol. 11, pp. 1-11, Pergamon Press Ltd, 1980.
- [2] Hoang Van Tung and Nguyen Dinh Duc, "Nonlinear Analysis of Stability for Functionally Graded Plates Under Mechanical and Thermal Loads", *Composite Structures*, Vol 92, Pgs 1184-1191, 2010.
- [3] Hui-Shen Shen, "Functionally Graded Materials-Nonlinear Analysis of Plates and Shells", *CRC Press*, 2009.
- [4] Hui-Shen Shen, "Karman-Type Equations for a Higher-Order Shear Deformation Plate Theory and its Use in the Thermal Postbuckling Analysis", *Applied Mathematics and Mechanics*, (English Edition, Vol. 18, No.12, Dec 1997).
- [5] Kingery, C.N. and G. Bulmash, "Air-Blast Parameters from TNT Spherical Airburst and Hemispherical Surface Burst", ABRL-TR-02555, U.S. Army Ballistic Research Laboratory, Aberdeen Proving Ground, MD, April 1984.
- [6] Reddy, J.N., "Mechanics of Laminated Composite Plates and Shells - Theory and Analysis", 2nd Edition, *CRC Press*, 1997.
- [7] Touloukian, Y.S., "Thermophysical properties of high temperature solid materials", MacMillan, N.Y., 1967
- [8] Tso-Liang Teng, Cho-Chung Liang, and Ching-Cho Liao, "Transient Dynamic Large-Deflection Analysis of Panel Structure Under Blast Loading", *JSME International Journal*, Series A, Vol. 39, No. 4, 1996.
- [9] Xiao-Lin Huang and Hui-Shen Shen, "Nonlinear Vibration and Dynamic Response of Functionally Graded Plates in Thermal Environments", *International Journal of Solids and Structures*, Vol 41, Pgs 2403-2427, 2004.
- [10] Young-Wann Kim, "Temperature Dependent Vibration Analysis of Functionally Graded Rectangular Plates", *Journal of Sound and Vibration*, Vol. 248, Pgs 531-549, 2005.